

BLIND DECONVOLUTION OF IMAGES USING GABOR FILTERS AND INDEPENDENT COMPONENT ANALYSIS

Shinji Umeyama

Neuroscience Institute,
The National Institute of Advanced Industrial Science and Technology
Tsukuba Central 2, Tsukuba, Ibaraki, 305-8568 Japan
s.umeyama@aist.go.jp

ABSTRACT

Independent Component Analysis is a new data analysis method, and its computation algorithms and applications are widely studied recently. Most applications, however, are for the field of one-dimensional data analysis, e.g. sound data analysis, and few applications for two-dimensional data (e.g., image data) are studied. In this paper we give a new blind deconvolution algorithm for images. In our method, Gabor filters are applied to the blurred image, and their output images and the original blurred image are provided as input data of ICA. One of the separated components is a restored image. We give a few experiments for artificial data and an experiment of a real blurred image. We also give a simple model to explain the validity of our algorithm.

1. INTRODUCTION

The image restoration is to estimate an original image from the image degraded by blurring and noise. The degrading process is usually modeled as a convolution of a Point Spread Function (PSF) with an original image and an additive noise.

If a PSF is known in advance, a lot of restoration algorithms, such as a Wiener filter and a generalized inverse filter, are proposed and the restoration method is almost established. However, these algorithms work only when a PSF is known, and an estimation of a PSF is not easy in general except, for example, the case as a blurring produced by an uniform and one-directional movement of a camera.

On the other hand, several restoration algorithms without using an information about a PSF are also proposed. This kind of an algorithm restores an original image by simultaneously estimating an image and a PSF, and it is called a *blind deconvolution*. These algorithms iteratively estimate both an image and a PSF by using *a priori* constraints such as the non-negative property of an image and a PSF, the finiteness of the support area of the object in an image, or the symmetric shape of a PSF [1, 2, 6]. An another blind

deconvolution method is *Super Resolution*. Super resolution is a method to estimate a signal from the band limited observation data and has been studied in the signal processing field.

Blind deconvolution was developed mainly for restoration of images in astronomy. This is because an image of an astronomical body (a star) should be a point in principle and this information is very useful as a priori constraint of the estimation.

In the field of Independent Component Analysis blind deconvolution is a very popular topic and a lot of papers were already published [4]. However, almost all papers handle the blind deconvolution of one-dimensional data, such as sound signals. Few papers are written for the blind deconvolution of *images* [3]. We give here a new blind deconvolution method of images. In our method, Gabor filters are applied to a blurred image first, and their output images and the original blurred image are provided as input data of ICA. We use the on-line stochastic gradient algorithm for ICA, and by appropriately selecting a sign of learning parameter ICA estimates a deblurred image as the first independent component when the image come from a natural scene. No *a priori* constraint is used in the algorithm.

We give a few experiments for artificial data and an experiment of a real blurred image. We also give a simple model to explain the validity of our algorithm.

2. GABOR FILTERS

The Gabor filters have received considerable attention in the computer vision field since the characteristics of certain cells in the visual cortex of some mammals can be approximated by these filters. They realize multichannel filtering which decompose an input image into a number of filtered images. Each filtered image contain intensity variation over a narrow range of frequency and orientation [5].

Two dimensional Gabor filter is given as a product of a 2D Gaussian function and a plane wave propagating to

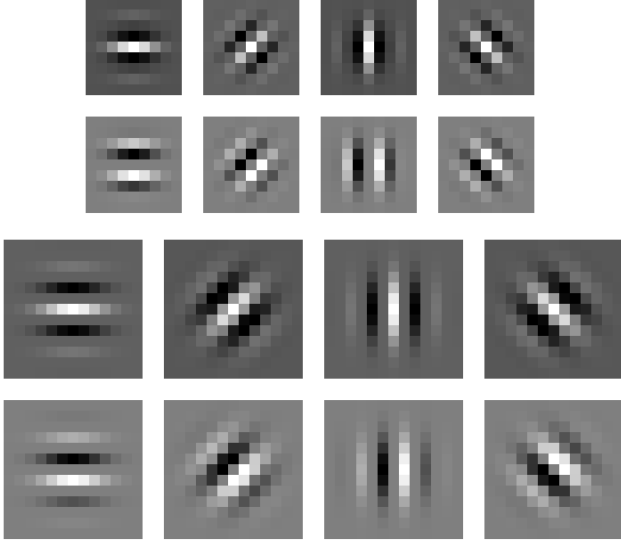


Fig. 1. Gabor filters

some direction on 2D plane. It is determined by the standard deviation of the Gaussian function and the propagating direction and the wave length of the plane wave. Since the standard deviation rules the extent of a Gaussian function, it also rules that of the Gabor filter. Thus the standard deviation is closely related to the wave length of a plane wave.

The 2D Gabor filter is defined as a complex function, and its real and imaginary part are used as two real filters. The following equations show 2D Gabor filters.

$$R(x, y; \nu, k) = \exp\left(-\frac{x^2 + y^2}{2\sigma_\nu^2}\right) \cdot \cos\left(\frac{\pi}{\sigma_\nu}(x \cos \phi_k + y \sin \phi_k)\right) \quad (1)$$

$$I(x, y; \nu, k) = \exp\left(-\frac{x^2 + y^2}{2\sigma_\nu^2}\right) \cdot \sin\left(\frac{\pi}{\sigma_\nu}(x \cos \phi_k + y \sin \phi_k)\right) \quad (2)$$

where

$$\sigma_\nu = (\sqrt{2})^{\nu+1} \quad (3)$$

$$\phi_k = \frac{\pi}{4}k \quad (4)$$

In the following experiments we set $\nu \in \{0, 1\}$ and $k \in \{0, 1, 2, 3\}$ as parameters, thus we use totally 16 Gabor filters. Fig.1 shows these filters as images. The upper two rows of Fig.1 are filters of $\nu = 0$, and the lower two rows are filters of $\nu = 1$. The first and third rows of images show Gabor filters corresponding to a real part, $R(x, y; \nu, k)$, and simulate the response of a simple neuron with a line detection ability. On the other hand, the second and fourth

rows show Gabor filters corresponding to an imaginary part, $I(x, y; \nu, k)$, and simulate the response of a simple neuron with an edge detection ability.

3. BLIND DECONVOLUTION OF A BLURRED IMAGE USING GABOR FILTERS

The shift-invariant blurring process is represented by a convolution of an original image $f(x, y)$ and a PSF $h(x, y)$ when a noiseless case. Thus a pixel value $g(x, y)$ of a blurred image is defined as a linear sum of pixel values of its neighboring pixels (discrete convolution).

$$g(x, y) = \sum_{s=-M}^M \sum_{t=-M}^M h(s, t)f(x + s, y + t) \quad (5)$$

When considering the Taylor expansion, the pixel value $f(x + s, y + t)$ of a neighboring pixel can be represented by a linear sum of the value $f(x, y)$ of the center pixel and its derivatives, such as $f_x(x, y)$ and $f_y(x, y)$.

$$f(x + s, y + t) = f(x, y) + sf_x(x, y) + tf_y(x, y) + \dots \quad (6)$$

Therefore the pixel value $g(x, y)$ can be approximated as follows by using Eq.(5) and Eq.(6).

$$g(x, y) = a_1f(x, y) + a_2f_x(x, y) + a_3f_y(x, y) + \dots \quad (7)$$

where

$$a_1 = \sum_{s=-M}^M \sum_{t=-M}^M h(s, t) \quad (8)$$

$$a_2 = \sum_{s=-M}^M \sum_{t=-M}^M sh(s, t) \quad (9)$$

$$a_3 = \sum_{s=-M}^M \sum_{t=-M}^M th(s, t) \quad (10)$$

Here we apply Gabor filters to the blurred image, which means that the original image is doubly convolved by a PSF and a Gabor filter. This is equivalent to a convolution of the original image and a function $h' = R * h$ or $h' = I * h$, where R and I are Gabor filters. Thus the discussion above similarly holds for the value $g'(x, y)$ of the filtered image.

$$g'(x, y) = a'_1f(x, y) + a'_2f_x(x, y) + a'_3f_y(x, y) + \dots \quad (11)$$

where

$$a'_1 = \sum_{s=-M}^M \sum_{t=-M}^M h'(s, t) \quad (12)$$

$$a'_2 = \sum_{s=-M}^M \sum_{t=-M}^M sh'(s, t) \quad (13)$$

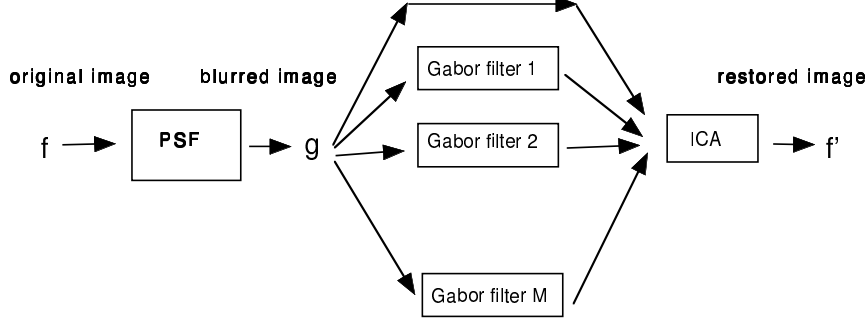


Fig. 2. Restoration by ICA and Gabor filters

$$a'_3 = \sum_{s=-M}^M \sum_{t=-M}^M th'(s, t) \quad (14)$$

The coefficient a'_i depends on the shape of the applied Gabor filter. If we change the Gabor filter, the coefficients also change.

This equation shows that the doubly blurred image g' is a mixture of the original image f and its derivative images, such as f_x and f_y , and the coefficients of the mixture are dependent on the applied Gabor filters. This discussion leads a possibility that an original image (and its derivatives) may be restored when we apply ICA to several doubly blurred images which undergo different Gabor filtering processes (Fig.2).

The restoration principle shown above does not constrain the shape of the filters. Any filter can be usable. However, we use the Gabor filters in this paper for two reasons. The first is that since the Gabor filters are similar to the first and second order differential filters, the output of the filters should be close to the first and the second derivative images. The restoration model above assumes the original image and its derivative images as independent components, thus we judged that the Gabor filters are suitable for the method. The second reason is that the hierarchical structure (Fig.1) of the Gabor filters may be useful for various degrees of blurring.

4. ICA ALGORITHM

The ICA algorithm used in the experiments is shown here briefly.

First the images (the blurred image and the output images of the Gabor filters) are transformed into vectors g_i by scanning them left-to-right and top-to-bottom manner. Here we center the data to make its mean zero. Then the data

matrix X is given as follows,

$$X = \begin{bmatrix} g_1^T \\ g_2^T \\ \dots \end{bmatrix}. \quad (15)$$

Next the column vectors x_j of X are whitened. We write z_j for the whitened data of x_j .

The element y_j of the first independent component y is given as the inner product of the weight vector w and the whitened data z_j .

$$y_j = w^T z_j \quad (16)$$

We use the on-line stochastic gradient algorithm to determine the weight vector w . The updating rule is as follows.

$$w \leftarrow w + \mu z_j \tanh w^T z_j \quad (17)$$

After updating, the length of w is normalized.

$$w \leftarrow \frac{w}{\|w\|} \quad (18)$$

If w is converged, this gives the first independent component.

The other independent components, if needed, are estimated using the same rule one after another. However, they are orthogonalized to the already estimated components at the normalization step. This kind of orthogonalization is called the deflationary orthogonalization [4].

The parameter μ in Eq.(17) is a learning parameter. The sign of this parameter must be set positive when estimating the independent component with a sub-Gaussian distribution, or set negative when estimating that with a super-Gaussian distribution. Since a crisp original image of a natural scene is usually sub-Gaussian and the derivative images are super-Gaussian (this is valid for images used in the experiment), the learning parameter for the first independent component (the restored image) was set positive and these of the remaining components negative.

We need only the first independent component (the restored image) for the blind deconvolution problem, thus ICA process is very simple.

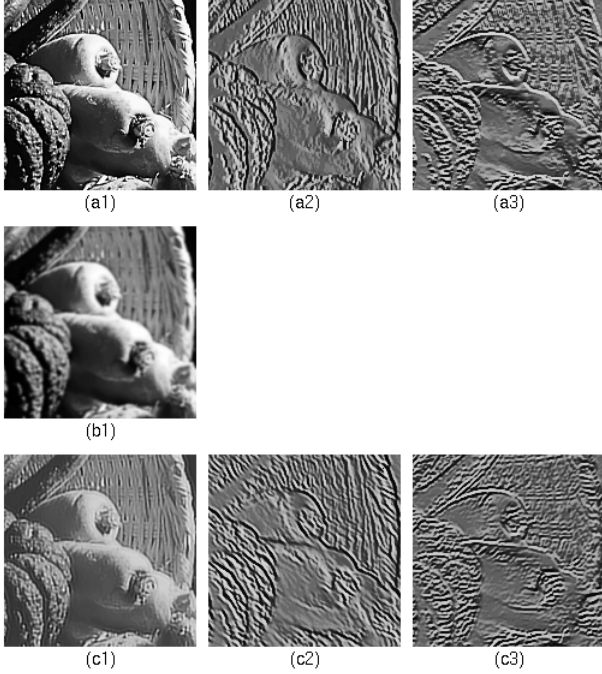


Fig. 3. Blind deconvolution results

5. RESTORATION EXPERIMENTS USING ARTIFICIAL DATA

The image restoration experiments based on the proposed method is given in this section. In the experiments the original crisp image is artificially blurred by a Gaussian filter, and several Gabor filters are applied to it. The outputs of the Gabor filters and the original blurred image are used as input data of ICA (Fig.2).

5.1. Basic experiment

The image shown in Fig.3(a1) was used as the original image. The size of the image is 160×160 . Fig.3(a2) and (a3) show the x -derivative and y -derivative images of the original image. The blurred image was created by applying a Gaussian filter to the original image. The parameters of the Gaussian filter were set as $\sigma_x = 1.0$ and $\sigma_y = 1.0$. We call this filter $G(1, 1)$.

The obtained blurred image is shown in Fig.3(b1). Gabor filters shown in Fig.1 were applied to it, and the output images of the filters and the original blurred image were fed to ICA. 17 independent components were estimated. The absolute value of the learning parameter was set 0.0001 for all components. This value is used for all experiments in this paper.

Fig.3(c1), (c2) and (c3) are obtained independent components which have high correlations with the original im-



Fig. 4. Original image

age (Fig.3(a1)), x -derivative image (Fig.3(a2)) and y -derivative image (Fig.3(a3)). The correlation coefficients with the original images are 0.967, 0.721, and 0.791, respectively. The correlation coefficient between the blurred image (Fig.3(b1)) and the original image is 0.920. This experiment shows that the proposed method gives a good restoration result ($0.920 \rightarrow 0.967$) even when the blurring process is unknown, and ICA gives not only the original images but its derivative images as the restoration model supposes.

5.2. Restoration experiment for various shapes of the blurring kernel

Here we applied the method to the blurred images which are generated by various shapes of the blurring kernel to show the adaptive behavior of the proposed method for the various blurring processes. The original image is given in Fig.4. We applied five kinds of Gaussian filters ($G(1,1)$, $G(2,2)$, $G(1,2)$, $G(2,1)$, and $G(1,3)$) to this image and got blurred images shown in the second row of Fig.5 ((a2),(b2),(c2),(d2), and (e2)). Fig.5 also shows the shapes of the applied Gaussian filters in the first row ((a1),(b1),(c1),(d1),and (e1)).

Each blurred image was translated by 16 Gabor filters of Fig.1, and the output of Gabor filters and the original blurred image were fed to ICA. The obtained restored images are given in the third row of Fig.5 ((a3),(b3),(c3),(d3), and (e3)).

Table.1 summarizes the correlation coefficients. The second column of Table.1 gives the correlation coefficients between the original image and the blurred image, and the third column gives the correlation coefficients between the original image and the restored image by ICA.

This experiment shows that the proposed method works well for different shapes of the blurring process.

Lastly we computed the regression coefficients (the regression mask) from a local window area (13×13) in the restored image to the center pixel value of the corresponding area in the blurred image. If we use the original image instead of the restored image in this computation, apparently we get the PSF of the blurring process. Thus this computation gives an estimation of the PSF of each experiment. The

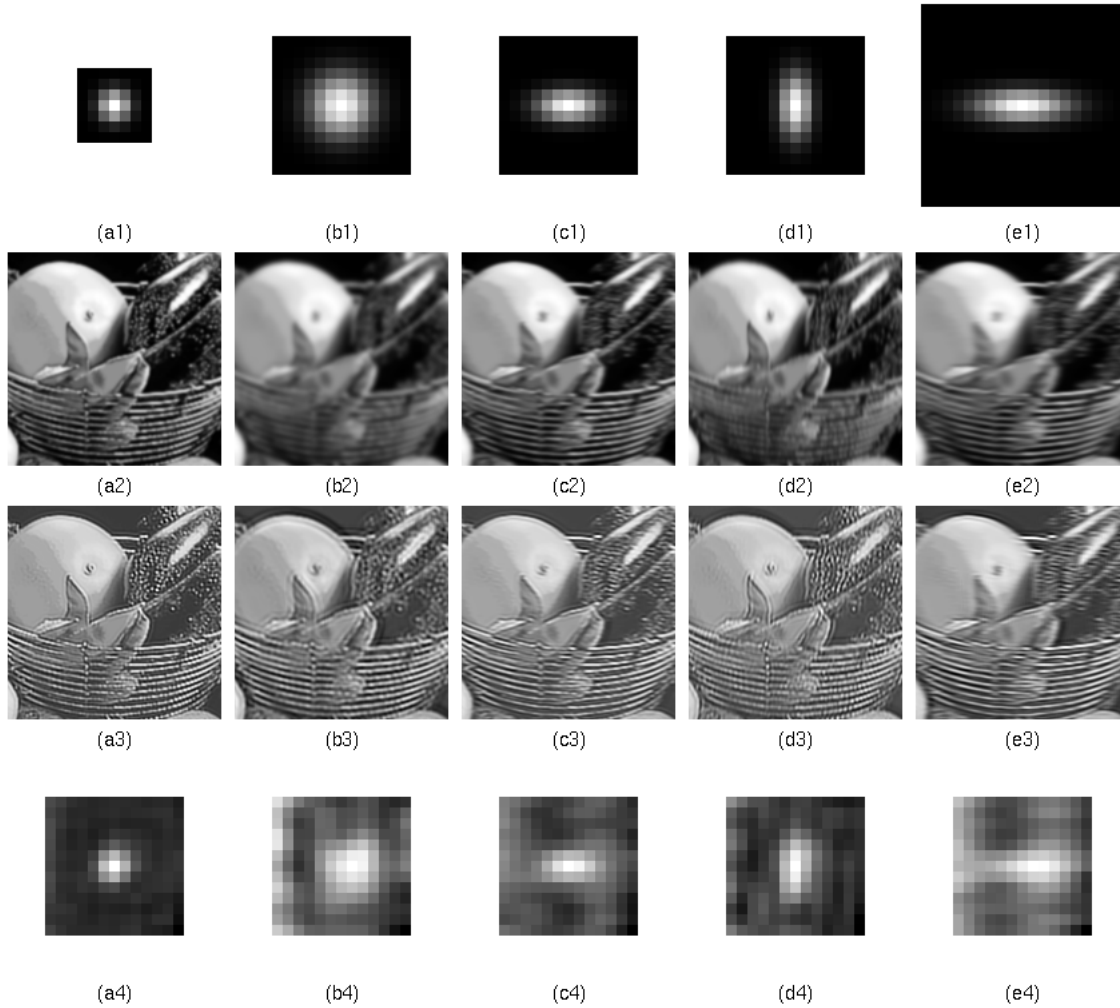


Fig. 5. Blind deconvolution results for various PSF's

result is shown in Fig.5 (a4), (b4), (c4), (d4), and (e4). The estimation is fairly good when comparing them with the true PSF (the first row of Fig.5).

Blur size	Blurred	Restored
(1,1)	0.871	0.957
(2,2)	0.756	0.879
(1,2)	0.836	0.919
(2,1)	0.774	0.896
(1,3)	0.810	0.890

Table 1. Correlation coefficients

6. RESTORATION OF A REAL BLURRED IMAGE

Here we applied the proposed method to a real blurred image. The image of some books on a shelf was captured by a digital camera. The focus of the image was intentionally shifted. The image is given in Fig.6(a1).

This image is translated by 16 Gabor filters of Fig.1, and the output of Gabor filters and the original blurred image were fed to ICA. The obtained restored image is given in Fig.6(a2). Some characters which we cannot recognize in the blurred image at all are now readable.

The proposed method assumes that a PSF is uniform throughout the image. This assumption does not hold com-

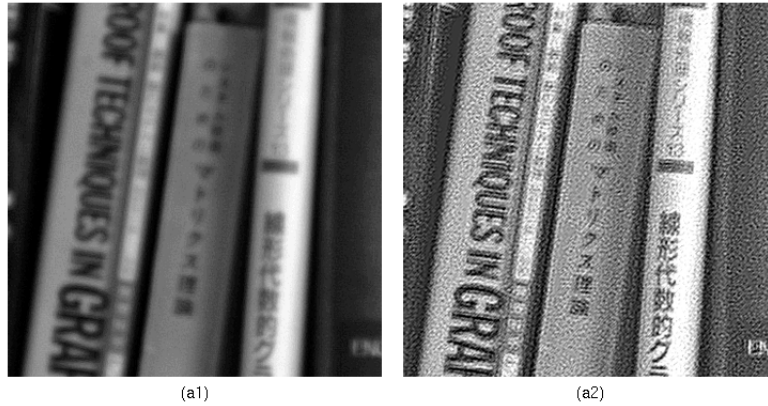


Fig. 6. Deblurring result of a real image

pletely in this experiment since the locations of the books are slightly different on a shelf. However, the method works approximately for this extent of nonuniformity. We need another approach to restore a blurred image including several objects of different distances, such as a landscape.

7. CONCLUSION

We proposed a new blind deconvolution method of images. In our method, Gabor filters are applied to a blurred image first, and their output images and the original blurred image are fed to ICA. We use the on-line stochastic gradient algorithm for ICA. No *a priori* constraint to estimate a PSF is used in the algorithm. We gave a few experiments for artificial data and an experiment of a real blurred image. We also gave a simple model to explain the validity of our algorithm.

The followings are the future work.

Gabor filters have a hierarchical structure. We may be able to utilize this property to restore the images of various blurring sizes adaptively. We also need to investigate the sensitiveness of the proposed algorithm to the noise.

8. REFERENCES

- [1] G.R. Ayers and J.C. Dainty, "Iterative blind deconvolution method and its applications", *Optics Letters*, vol.13, No.7, pp.547-549, 1988.
- [2] T.F. Chan and C-K Wong, "Total variation blind deconvolution", *IEEE Trans. on Image Processing*, vol.7, No.3, pp.370-375, 1998.
- [3] A. Cichocki and A. Amari, *Adaptive Blind Signal and Image Processing*, John-Wiley & Sons, 2002.
- [4] A.Hyvärinen, J. Karhunen, and E. Oja, *Independent Component Analysis*, A Wiley-International Publication, 2001.
- [5] A.K.Jain and S.K. Bhattacharjee, "Address block location on envelopes using Gabor filters", *Pattern Recognition*, Vol.25, No.12, pp.1459-1477, 1992.
- [6] R.G. Lane, "Blind deconvolution of speckle images", *J. Opt. Soc. Am*, vol.9, pp.1508-1514, 1992.